

Residual Energy Harvesting from Light Transients Using Hematite as an Intrinsic Photocapacitor in a Symmetrical Cell

Nicole S. van Leeuwen,^{†,‡} Burgert Blom,[‡] Mengying Xie,[§] Vana Adamaki,[§] Chris R. Bowen,[§] Moisés A. de Araújo,^{||} Lucia H. Mascaro,^{||} Petra J. Cameron,[†] and Frank Marken^{*,†}

[†]Department of Chemistry, University of Bath, Claverton Down, Bath BA2 7AY, United Kingdom

[‡]Maastricht Science Programme, Maastricht University, Maastricht 6200 MD, The Netherlands

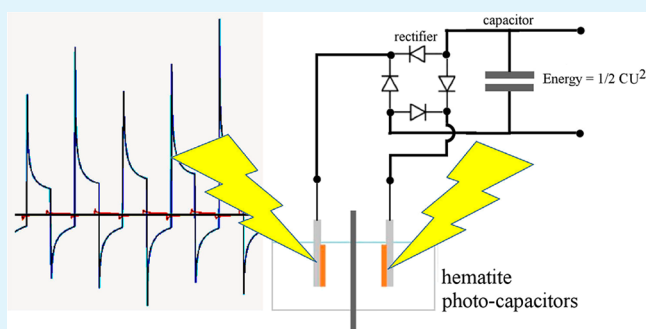
[§]Department of Mechanical Engineering, University of Bath, Claverton Down, Bath BA2 7AY, United Kingdom

^{||}Department of Chemistry, San Carlos Federal University, Rod. Washington Luiz, km235, CEP 13565-905, São Carlos, SP, Brazil

Supporting Information

ABSTRACT: Hematite as a sustainable photoabsorber material offers a band gap close to 2 eV and photoanode characteristics, but usually requires additional catalysts to enhance surface redox chemistry during *steady state* light energy harvesting for water splitting. Here, for a highly doped hematite film, sufficient intrinsic photocapacitor behavior is reported for the conversion of *light transients* into energy. Residual energy is harvested in a symmetric architecture with two opposing mesoporous hematite films on conductive glass. Transient light energy harvesting is shown to occur without the need for water splitting.

KEYWORDS: photocapacitance, charge carrier, flicker light, time constant, energy harvesting cycle, energy conversion



Ambient energy harvesting technologies have emerged for mechanical vibrations (based on piezoelectrics) and variations of temperature with time (based on pyroelectrics), as well as for static light energy.^{1,2} Often the harvesting mechanism is based on a cycle of high/low mechanical pressure or high/low temperature applied in an alternating fashion to create ac power output that is often rectified and stored in a capacitor. Similarly, for light energy harvesting a light-on/light-off cycle could be imagined. In nature, a similar principle of intermittent energy storage is realized in photosynthesis, which is based on a diurnal light–dark cycle with continuous energy production even during the night-time phase. The “dark process” relies on stored energy and operates out-of-phase to the “light process”. Recently, new artificial systems mimicking this behavior have been proposed on the basis of stored charge carriers or “photocapacitance”, for example, in photocatalytic hydrogen production.³

Photocapacitor behavior was initially proposed and developed by Miyasaka^{4,5} which coupled a mesoporous titania photoactive film with a porous carbon capacitive layer. Materials for typical photocapacitors are mainly based on carbon,⁶ PANI,⁷ silicon,⁸ or PEDOT⁹ and are usually configured as a separate photoactive absorber layer and capacitor layer. A review in this area has appeared recently.¹⁰ However, it is rare for capacitance to be directly integrated into the light absorber layer, although related biophotocapacitor systems have been described recently.¹¹ In semiconductor electrodes, intrinsic photocapacitance is usually an unwanted

component in solar cells as it can lead to “reversible charging” of traps as opposed to the “irreversible charging” required for flow of electricity and energy production. The irreversible surface chemical step of water oxidation links electrical ionic current flow and leads to internal rectification and energy harvesting. It is shown here that a reversible charging/discharging effect induced by intrinsic photocapacitance in highly doped hematite in the presence of a transient/pulsed light source can also be used in energy harvesting when rectified externally (see Figure 1). Rules for this ac energy harvesting still need to emerge. However, similar approaches have been used in pyroelectric devices for harvesting residual heat since thermal cycling leads to reversible charging/discharging as a result of an increase and decrease of the polarization of a material.¹²

The net energy harvesting efficiency under “steady state” conditions could in principle be comparable to that under “transient” or cyclic conditions (given similar light absorption coefficients and recombinational losses), although very different parameters need to be optimized in the two approaches. The ability to store charges or “intrinsic photocapacitance” as well as the charging/discharging time constant are crucial in the latter case. The switching frequency of the light source will therefore be of importance.

Received: October 14, 2017

Accepted: December 12, 2017

Published: December 12, 2017

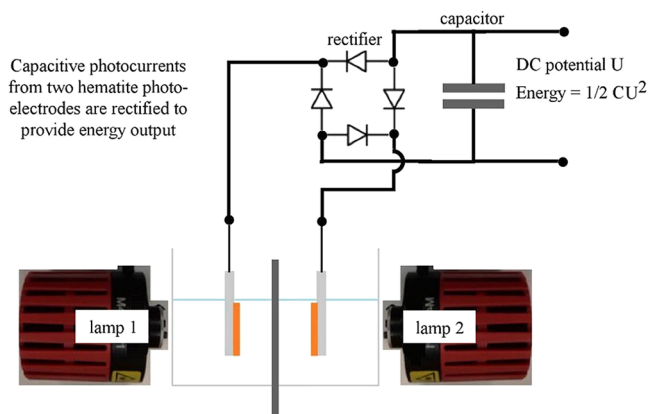


Figure 1. Schematic of a symmetric electrochemical cell with two hematite-coated FTO electrodes immersed in aqueous 0.1 M NaOH. Lamp 1 and lamp 2 apply synchronized on–off cycles so that one electrode is always illuminated and the other dark. An external rectifier converts the ac output to dc energy.

For hematite, the intrinsic capacitance (or redox pseudocapacitance) response has been shown to be associated with surface states and exploited in light or potential modulated adsorption spectroscopy (LMAS or PMAS).¹³ Hematite has often been highlighted as an abundant and sustainable raw material with potential for applications as a photoabsorber.^{14–16} Hematite offers a band gap of typically 2 eV with good characteristics as a photoanode for water splitting.^{17–19} Problems in performance are linked mainly to recombination of photogenerated charge carriers in the bulk and at surface states,²⁰ slow surface kinetics associated with the formation of oxygen,¹³ and poor electrical conductivity.^{21–23} In this study fluorine-doped tin oxide (FTO) electrodes were used as a substrate and hematite films prepared following the spin-coating methodology introduced by Souza et al.²⁴ (For experimental information please see [Supporting Information](#).) A notable modification to the preparation method here is a shorter calcination/annealing time to provide a more highly doped (and more capacitive) hematite product of semi-transparent reddish-brown coloration (see inset in [Figure S1A](#)). The cross-sectional image of a hematite spin-coated electrode after annealing is shown in [Figure S1A](#). Top view images reveal only a very smooth layer (not shown). The cross-section of the sample shows a thin hematite layer of approximately 600 nm thickness on an equally thick FTO support. The hematite layer is composed of smaller nanoparticles of about 40 nm diameter. XRD data ([Figure S1B](#)) confirm the formation of hematite without any other iron oxide phases being identified. However, the crystallinity of samples was variable, with minor unidentified signals at 28.47° and 42.57°.

Characteristic Raman peaks for hematite ([Figure S1C](#)) are anticipated²⁵ at 225, 247, 293, 299, 412, 498, and 613 cm^{-1} . As shown in [Figure S1C](#), only five main signals are present at 215, 243, 279, 401, 493, and 599 cm^{-1} . These signals demonstrate the presence of hematite, and the small shift in signals can be attributed to the use of a higher laser power.²¹ In addition, a strong peak at 1314 cm^{-1} commonly encountered in hematite is visible and may be associated with an artifact caused by antiferromagnetic behavior of $\alpha\text{-Fe}_2\text{O}_3$.²¹ Partially covered by this signal, a smaller peak around 1100 cm^{-1} is visible. A broad signal at 2400–2600 cm^{-1} and a smaller bump at 814 cm^{-1} are

also visible and possibly linked to the presence of FTO underneath the hematite layer. Some of these signals could be associated with the presence of residual carbon inclusions due to incomplete calcination of the carbon-rich precursor material. Carbon containing materials usually display a strong signal in the 1300–1350 cm^{-1} range for sp^3 hybridized carbon.²⁶ The color of films and cut off wavelength at 592 nm are consistent with hematite and a band gap of 2 eV.²¹

Voltammetry experiments were performed in aqueous 0.1 M NaOH initially in the absence of light which revealed the onset of a reduction at -0.2 V versus SCE (see [Figure 2A](#)).

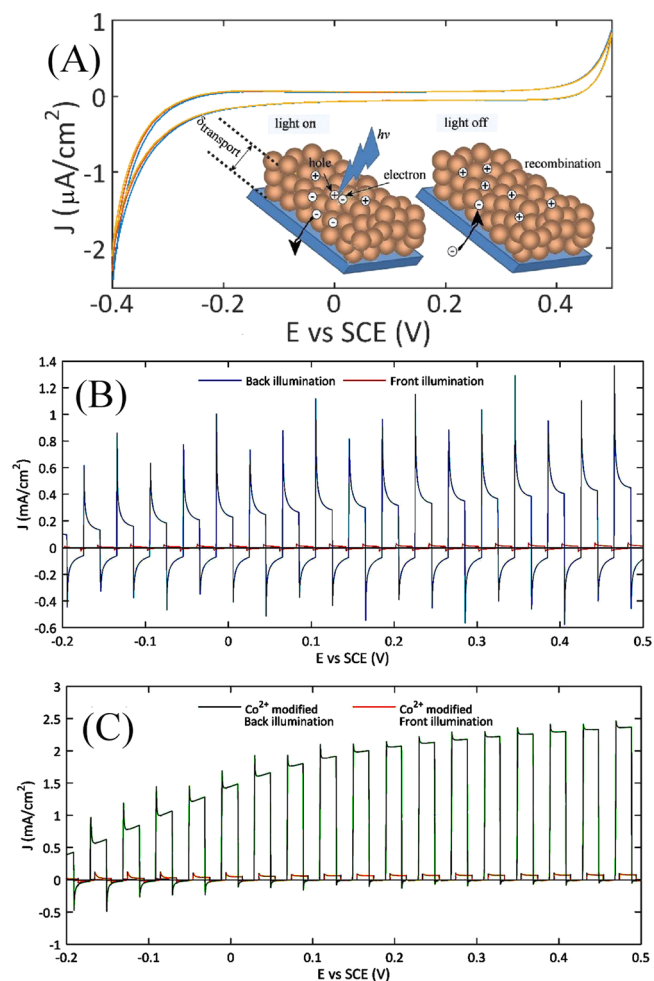


Figure 2. (A) Schematic of light-on and light-off processes in mesoporous hematite. Cyclic voltammograms (3 consecutive cycles, scan rate 20 mVs^{-1}) for hematite film immersed in 0.1 M NaOH. (B) Linear scan voltammogram (scan rate 20 mVs^{-1} ; pulsed LED light; 1 s on 1 s off pulses; irradiance ca. 100 mW cm^{-2}) for a hematite film immersed in aqueous 0.1 M NaOH. (C) As before, but with Co(II)-catalyst-coated hematite.

Therefore, further experiments were initiated at -0.2 V versus SCE. Next, linear sweep voltammograms were recorded in the presence of pulsed light, as shown in [Figure 2B](#). Photocurrent density measurements were performed with back and with front illumination. Back illumination can be seen to produce considerably higher photocurrents. With back illumination, charge carriers are generated closer to the FTO–hematite interface, which facilitates their extraction into the FTO layer and thereby reduces the extent of transport/recombinational

losses. In hematite films, light has a penetration depth of approximately 500 nm thickness.¹⁷ With an estimated thickness of 600 nm for these films, front illumination light may not penetrate deep enough for charge separation to be effectively collected at the interface. The transport layer for electrons, $\delta_{\text{transport}}$ (see inset Figure 2A), is likely to be only a fraction of the total thickness. The reaction layer, $\delta_{\text{reaction}} = (D_e/k_{\text{surface}})^{0.5}$, can be defined on the basis of the electron diffusivity and the first order surface reaction for the water splitting process involving holes at the hematite surface. This is likely to be more extended in the case of low surface reactivity; i.e., the process becomes transport limited, and current spikes are observed.

Transient photocurrents for both back and front illumination show a characteristic light-on spike of anodic current, which is followed by a decay to give a steady state current density. When the light is switched off, a cathodic current spike is observed. The anodic spike arises from charge separation and rapid electron diffusion toward/into the FTO–hematite interface.^{27,28} The fast decay following the anodic spike is usually associated with slow oxygen evolution kinetics and the presence of surface traps (pseudocapacitance). Trap concentrations can be enhanced due to defects on the surface or in the crystal structure often associated with a low degree of crystallinity and purity of the hematite film.^{23,29} When the light is turned off, the generation of mobile charges is interrupted, and electrons flow back and undergo recombination with holes, which can occur by reduction of the previously oxidized surface traps. This process induces a cathodic light-off current spike.

Spin-coated electrodes were found to exhibit current spikes of typically 1.0 mA cm^{-2} and steady state currents of typically 0.5 mA cm^{-2} at 0.4 V versus SCE. Some variation in photocurrent between samples was observed, but the behavior explained above was common to all samples. Even though the same procedure was applied for each spin-coated sample, these variations suggest that photoactivity is highly sensitive to layer composition and calcination conditions. More extended calcination resulted in less cathodic light-off current responses. Harvesting energy from the steady state water splitting response of the films in Figure 2B is inefficient because of extensive charging and slow oxygen evolution. Traditionally, a catalyst such as Co(II) has been proposed as a way to improve performance. Figure 2C shows data for hematite films with Co(II)-coated hematite following the procedure suggested by Zhong et al.³⁰ Much improved water splitting responses (higher steady state photoanodic currents and less evidence for light-on/off transients) are observed in particular for back illumination.

The production of oxygen at the hematite surface by photocatalytic water splitting introduces irreversibility (rectification via semiconductor interfaces and chemistry) to allow conversion of light energy into chemical energy. The transient or intrinsic photocapacitive behavior of the hematite electrodes in Figure 2B is usually considered a drawback of photoanode materials due to the considerable drop in photocurrent as a result of charging of the semiconductor interface and extensive charge recombination in trap states. However, energy stored in this intrinsic capacitive charging process can be extracted by switching the light source on and off. The resulting ac current output can be rectified and accumulated/rectified in an external capacitor as shown in Figure 1. Instead of employing a single hematite photoanode with a second nonphotoactive electrode, here two hematite electrodes are used in tandem with one light source being switched on simultaneously to the second being

switched off. As a result, the voltage between the two electrodes will change with time, as well as the charge state, to generate current.

Typical chronopotentiometry (zero current) data for light-on and light-off transients for a single hematite electrode are shown in Figure 3A. Back illumination can be seen to result in

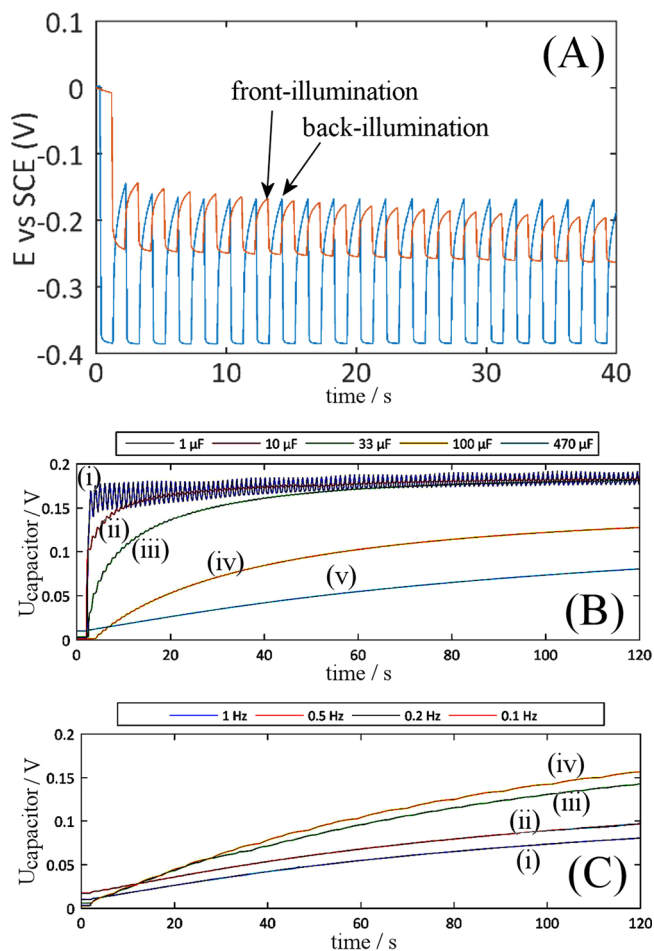


Figure 3. (A) Chronopotentiometry (zero current) for a hematite electrode in 0.1 M NaOH under front (orange) and back (blue) illumination conditions (irradiance ca. 100 mW cm^{-2}). (B) Capacitor charging potential (light switching frequency 1 Hz) as a function of time for external capacitance (i) 1, (ii) 10, (iii) 33, (iv) 100, and (v) 470 μF . (C) As before, but for 470 μF capacitance and (i) 1, (ii) 0.5, (iii) 0.2, (iv) 0.1 Hz light switching frequency.

more pronounced changes in potential with approximately 0.2 V voltage span between light-on and light-off conditions. When considering two coupled hematite electrodes, as shown in Figure 1, the complexity of resolving processes at individual hematite electrodes under these conditions is beyond the scope of this report. However, preliminary proof-of-principle data sets in Figure 3B demonstrate that the potential U (measured across an external capacitor) is increased when switching the light sources at a 1 Hz frequency. A small external capacitor of 1 μF (see circuit in Figure 1) rapidly charges to approximately $U = 0.18 \text{ V}$ (corresponding to an energy of $1/2CU^2$) but then rapidly loses energy during the second part of the cycle. This is due to one of the two hematite electrodes being less effective, thereby leading to a modulation. The “potential ceiling” at 0.18 V (compare 0.2 V transients in Figure 3A) suggests that at this relative voltage the loss of charge at the semiconductor/

electrolyte interface is increased so much (possibly due to oxygen evolution or reduction) that further charging is impossible. Water splitting chemistry at more positive potentials now may be considered an unwanted side reaction causing energy losses. In order to suppress the “voltage ceiling” effect, increasing the external capacitor value (C) to 100 or 470 μF is effective (see Figure 3Biv,v, since this leads to a lower voltage for a given charge (Q) level, since $Q = C \times U$). When compared to the experiment with the 1 μF capacitor, the 470 μF capacitor provides an approximately 200-fold increase in energy harvesting after 120 s.

Cuadras et al.³¹ provide an approximate analysis of the ceiling voltage U_{ceiling} based on the assumption of ideal diodes, Q the charge generated each cycle, Q_{leak} the charge leaked over a cycle (here mainly due to oxygen evolution), U_{diode} the voltage dropped across the diodes (here a very significant factor), and C_{photo} here the intrinsic photocapacitance (see eq 1).

$$U_{\text{ceiling}} = \frac{Q - Q_{\text{leak}} - 4U_{\text{diode}}C_{\text{photo}}}{2C_{\text{photo}}} \quad (1)$$

Clearly, the voltage U_{ceiling} is not dependent on the external capacitor (see Figure 3B), but the energy harvested is directly proportional to the external capacitor. The parameter Q_{leak} here is mainly associated with the charge transfer resistance for oxygen evolution and is crucial in limiting the voltage and limiting energy harvesting. The voltage U_{diode} as well as Q_{leak} should ideally be small so that ultimately $U_{\text{ceiling}} = Q/2C_{\text{photo}}$. Both are considerable in the work reported here, and therefore, further improvements are likely. The charge generated in the energy harvesting cycle should be high (compared to Q_{leak}). Other components to consider are the effects of frequency and wave shape. Any deviation from an ideal square waves will cause losses.

The frequency of light source switching offers a further parameter to optimize the energy harvesting process. High frequencies lead to energy losses due to an insufficient photovoltage being built up, and low frequencies lead to losses due to more recombination and water splitting. The plots in Figure 3B can be interpreted as square root of energy versus time (with a fixed capacitance), and clearly lower frequencies are beneficial. Even lower frequencies (not shown) caused loss in performance, and the optimum light switching frequency here was 0.1 Hz. The energy stored in 60 s reaches 3.3 μJ corresponding to 0.05 $\mu\text{W cm}^{-2}$ (or 0.5 μA at 0.1 V). This energy output seems low when compared to the light energy absorbed (assuming ca. 100 mW cm^{-2} LED intensity), but is comparable to the output of other devices for residual energy harvesting,³² and improvements will be possible. In particular, surface blocking layers could be applied to the hematite surface to further suppress water splitting and to allow higher voltages to build up on the capacitor. Although water and particularly protons may be important in the photocapacitance effect, it may also be possible to operate similar devices under nonaqueous conditions. Furthermore, better matching of applied frequency and internal photocapacitance leakage resistance will be important. Also, the stability of photocapacitance responses under light transient conditions for these hematite electrodes in aqueous 0.1 M NaOH appears limited and will need further attention.

In conclusion, highly doped pseudocapacitive hematite thin film electrodes were successfully synthesized using a spin-coating deposition method adapted from Souza et al.²⁴ using

the citric acid polymerization approach. The resulting electrodes were semitransparent and of a dark-red-orange color and based on approximately 600 nm thick hematite. Doping-enhanced intrinsic photocapacitance was observed compared to that observed for more thoroughly calcined hematite. Transient photocurrent behavior has been exploited with an external rectifier circuit to provide an example of an “ac solar cell” for residual energy harvesting. Energy loss mechanisms have been identified primarily on the basis of the voltage drop in the diode rectifier circuit (to be dealt with in future by working at higher voltages) and due to residual water splitting activity (to be dealt with in future by improving hematite surface chemistry and by changing the electrolyte). The frequency for energy harvesting to maximize was shown in this case to be 0.1 Hz. This optimum frequency (or time constant) will need to be adjusted depending on application to diurnal (for solar light harvesting) or much faster to 50 Hz (for harvesting from artificial light sources). More work will also be required to explore/improve the principal limits of ac mode light harvesting devices compared to dc mode light harvesting cells.

■ ASSOCIATED CONTENT

📄 Supporting Information

The Supporting Information is available free of charge on the ACS Publications website at DOI: 10.1021/acsam.7b00035.

(PDF)

■ AUTHOR INFORMATION

Corresponding Author

*E-mail: F.Marken@bath.ac.uk.

ORCID

Petra J. Cameron: 0000-0001-8182-5546

Frank Marken: 0000-0003-3177-4562

Notes

The authors declare no competing financial interest.

■ ACKNOWLEDGMENTS

N.S.v.L. and B.B. thank the Maastricht Science programme for support. C.R.B., M.X., and V.A. acknowledge funding from the European Research Council under the European Union's Seventh Framework Programme (FP/2007-2013)/ERC Grant Agreement 320963 on Novel Energy Materials, Engineering Science and Integrated Systems (NEMESIS). M.A.d.A., L.H.M., and F.M. thank CAPES (PVE 71/2013) 327 and FAPESP (2013/07296-2) and CNPq (472384/2012-0) for financial support. We thank Professor Laurie M. Peter for discussion and support.

■ REFERENCES

- (1) Dunn, S. Routes to Energy Conversion with Functional Oxide Films and Nanostructures, a Short Review. *Thin Solid Films* **2016**, *601*, 59–62.
- (2) Bowen, C. R.; Taylor, J.; LeBoulbar, E.; Zabek, D.; Chauhan, A.; Vaish, R. Pyroelectric Materials and Devices for Energy Harvesting Applications. *Energy Environ. Sci.* **2014**, *7*, 3836–3856.
- (3) Lau, V. W. H.; Klose, D.; Kasap, H.; Podjaski, F.; Pignie, M. C.; Reisner, E.; Jeschke, G.; Lotsch, B. V. Dark Photocatalysis: Storage of Solar Energy in Carbon Nitride for Time-Delayed Hydrogen Generation. *Angew. Chem., Int. Ed.* **2017**, *56*, 510–514.
- (4) Miyasaka, T.; Murakami, T. N. The Photocapacitor: An Efficient Self-charging Capacitor for Direct Storage of Solar Energy. *Appl. Phys. Lett.* **2004**, *85*, 3932–3934.

- (5) Miyasaka, T.; Kijitori, Y.; Ikegami, M. Plastic Dye-sensitized Photovoltaic Cells and Modules Based on Low-temperature Preparation of Mesoscopic Titania Electrodes. *Electrochemistry* **2007**, *75*, 2–12.
- (6) Lee, F. W.; Ma, C. W.; Lin, Y. H.; Huang, P. C.; Su, Y. L.; Yang, Y. J. A Micromachined Photo-Supercapacitor Integrated with CdS-Sensitized Solar Cells and Buckypaper. *Sens. Mater.* **2016**, *28*, 749–756.
- (7) Yang, Z. B.; Li, L.; Luo, Y. F.; He, R. X.; Qiu, L. B.; Lin, H. J.; Peng, H. S. An Integrated Device for Both Photoelectric Conversion and Energy Storage Based on Free-standing and Aligned Carbon Nanotube Film. *J. Mater. Chem. A* **2013**, *1*, 954–958.
- (8) Cohn, A. P.; Erwin, W. R.; Share, K.; Oakes, L.; Westover, A. S.; Carter, R. E.; Bardhan, R.; Pint, C. L. All Silicon Electrode Photocapacitor for Integrated Energy Storage and Conversion. *Nano Lett.* **2015**, *15*, 2727–2731.
- (9) Xu, J.; Ku, Z. L.; Zhang, Y. Q.; Chao, D. L.; Fan, H. J. Integrated Photo-Supercapacitor Based on PEDOT Modified Printable Perovskite Solar Cell. *Adv. Mater. Technol.* **2016**, *1*, 1600074.
- (10) Liu, R. Y.; Liu, Y. Q.; Zou, H. Y.; Song, T.; Sun, B. Q. Integrated Solar Capacitors for Energy Conversion and Storage. *Nano Res.* **2017**, *10*, 1545–1559.
- (11) Gonzalez-Arribas, E.; Aleksejeva, O.; Bobrowski, T.; Toscano, M. D.; Gorton, L.; Schuhmann, W.; Shleev, S. Solar Biosupercapacitor. *Electrochem. Commun.* **2017**, *74*, 9–12.
- (12) Wang, Q. P.; Zhang, X.; Bowen, C. R.; Li, M. Y.; Ma, J. H.; Qiu, S. Y.; Liu, H.; Jiang, S. L. Effect of Zr/Ti Ratio on Microstructure and Electrical Properties of Pyroelectric Ceramics for Energy Harvesting Applications. *J. Alloys Compd.* **2017**, *710*, 869–874.
- (13) Cummings, C. Y.; Marken, F.; Peter, L. M.; Upul Wijayantha, K. G.; Tahir, A. A. New Insights into Water Splitting at Mesoporous α -Fe₂O₃ Films: A Study by Modulated Transmittance and Impedance Spectroscopies. *J. Am. Chem. Soc.* **2012**, *134*, 1228–1234.
- (14) Wheeler, D. A.; Wang, G. M.; Ling, Y. C.; Li, Y.; Zhang, J. Z. Nanostructured Hematite: Synthesis, Characterization, Charge Carrier Dynamics, and Photoelectrochemical Properties. *Energy Environ. Sci.* **2012**, *5*, 6682–6702.
- (15) Peter, L. M. Energetics and Kinetics of Light-driven Oxygen Evolution at Semiconductor Electrodes: the Example of Hematite. *J. Solid State Electrochem.* **2013**, *17*, 315–326.
- (16) Barroso, M.; Mesa, C. A.; Pendlebury, S. R.; Cowan, A. J.; Hisatomi, T.; Sivula, K.; Grätzel, M.; Klug, D. R.; Durrant, J. R. Dynamics of Photogenerated Holes in Surface Modified α -Fe₂O₃ Photoanodes for Solar Water Splitting. *Proc. Natl. Acad. Sci. U. S. A.* **2012**, *109*, 15640–15645.
- (17) Sivula, K.; Le Formal, F.; Grätzel, M. Solar Water Splitting: Progress Using Hematite (α -Fe₂O₃) Photoelectrodes. *ChemSusChem* **2011**, *4*, 432–449.
- (18) Glasscock, J. A.; Barnes, P. R. F.; Plumb, I. C.; Bendavid, A.; Martin, P. J. Structural, Optical and Electrical Properties of Undoped Polycrystalline Hematite Thin Films Produced Using Filtered Arc Deposition. *Thin Solid Films* **2008**, *516*, 1716–1724.
- (19) Hamann, T. W. Splitting Water with Rust: Hematite Photoelectrochemistry. *Dalton Trans.* **2012**, *41*, 7830–7834.
- (20) Upul Wijayantha, K. G.; Saremi-Yarahmadi, S.; Peter, L. M. Kinetics of Oxygen Evolution at α -Fe₂O₃ Photoanodes: a Study by Photoelectrochemical Impedance Spectroscopy. *Phys. Chem. Chem. Phys.* **2011**, *13*, 5264–5270.
- (21) Tamirat, A. G.; Rick, J.; Dubale, A. A.; Su, W. N.; Hwang, B. J. Using Hematite for Photoelectrochemical Water Splitting: a Review of Current Progress and Challenges. *Nanoscale Horiz* **2016**, *1*, 243–267.
- (22) Kennedy, J. H.; Frese, K. W. Photo-Oxidation of Water at α -Fe₂O₃ Electrodes. *J. Electrochem. Soc.* **1978**, *125*, 709–714.
- (23) Le Formal, F.; Sivula, K.; Grätzel, M. The Transient Photocurrent and Photovoltage Behavior of a Hematite Photoanode under Working Conditions and the Influence of Surface Treatments. *J. Phys. Chem. C* **2012**, *116*, 26707–26720.
- (24) Souza, F. L.; Lopes, K. P.; Nascente, P. A. P.; Leite, E. R. Nanostructured Hematite Thin Films Produced by Spin-coating Deposition Solution: Application in Water Splitting. *Sol. Energy Mater. Sol. Cells* **2009**, *93*, 362–368.
- (25) deFaria, D. L. A.; Venancio Silva, S.; deOliveira, M. T. Raman Microspectroscopy of some Iron Oxides and Oxyhydroxides. *J. Raman Spectrosc.* **1997**, *28*, 873–878.
- (26) Ferrari, A. C.; Robertson, J. Interpretation of Raman Spectra of Disordered and Amorphous Carbon. *Phys. Rev. B: Condens. Matter Mater. Phys.* **2000**, *61*, 14095–14107.
- (27) Klahr, B.; Gimenez, S.; Fabregat-Santiago, F.; Bisquert, F.; Hamann, T. W. Electrochemical and Photoelectrochemical Investigation of Water Oxidation with Hematite Electrodes. *Energy Environ. Sci.* **2012**, *5*, 7626–7636.
- (28) Bondarchuk, A. N.; Peter, L. M.; Kissling, G. P.; Madrid, E.; Aguilar-Martinez, J. A.; Rymansaib, Z.; Irvani, P.; Gromboni, M.; Mascaro, L. H.; Walsh, A.; Marken, F. Vacuum-annealing Induces Sub-surface Redox-states in Surfactant-structured α -Fe₂O₃ Photoanodes Prepared by Ink-jet Printing. *Appl. Catal., B* **2017**, *211*, 289–295.
- (29) Le Formal, F.; Grätzel, M.; Sivula, K. Controlling Photoactivity in Ultrathin Hematite Films for Solar Water-Splitting. *Adv. Funct. Mater.* **2010**, *20*, 1099–1107.
- (30) Zhong, D. K.; Cornuz, M.; Sivula, K.; Grätzel, M.; Gamelin, D. R. Photo-assisted Electrodeposition of Cobalt-phosphate (Co-Pi) Catalyst on Hematite Photoanodes for Solar Water Oxidation. *Energy Environ. Sci.* **2011**, *4*, 1759–1764.
- (31) Cuadras, A.; Gasulla, M.; Ferrari, V. Thermal Energy Harvesting through Pyroelectricity. *Sens. Actuators, A* **2010**, *158*, 132–139.
- (32) Zhang, Y.; Xie, M. Y.; Roscow, J.; Bao, Y. X.; Zhou, K. C.; Zhang, D.; Bowen, C. R. Enhanced Pyroelectric and Piezoelectric Properties of PZT with Aligned Porosity for Energy Harvesting Applications. *J. Mater. Chem. A* **2017**, *5*, 6569–6580.